ASTRONOMY & ASTROPHYSICS
SUPPLEMENT SERIES

MAY 1987, PAGE 171

Astron. Astrophys. Suppl. Ser. **69,** 171-182 (1987)

Radio observations of the first ranked galaxies in A98, A115, A160, A278 and A568

G. Giovannini, L. Feretti and L. Gregorini

Dipartimento di Astronomia, Universita' di Bologna, Casella Postale 596, I-40100 Bologna, Italy
Istituto di Radioastronomia, Via Irnerio 46, I-40126 Bologna, Italy

Received October 6, accepted November 26, 1986

Summary. — We present VLA and WSRT data on 5 extended radio sources identified with first ranked galaxies in rich Abell clusters. The observing frequency is 1.4 GHz for A98, A160, A278, A568 and 4.9 GHz for A115, A160, A568. These sources show a variety of morphologies, ranging from head-tail type to extremely collimated jets. The trend of spectral index and polarization data are given, when possible. It seems likely that these sources are interacting with the ambient gas, which is revealed by X-ray observations.

Key words : clusters of galaxies — radio galaxies — first ranked galaxies — VLA maps — radio continuum.

1. Introduction.

An important approach to the study of the radio source phenomenon is a comparison of radio source morphologies found inside clusters of galaxies with those occurring outside. Bent or otherwise distorted structures are preferentially present in radio sources identified with galaxies belonging to clusters (e.g. Fanti, 1984). This fact is currently interpreted in terms of the interaction of the radio emitting plasma with the surrounding medium. Detailed study of the structure of the cluster radio galaxies must therefore lead to a better understanding of the formation and evolution of the radio source, and of the environment itself. Of particular importance is the radio study of the first ranked galaxies, since they are located in the cluster center and are the most massive and the brightest galaxies of the cluster.

In this context we present here new radio data on four extended radio sources identified with the first ranked galaxies of the Abell clusters 98, 160, 278 and 568. Furthermore some additional radio data are presented for the radio galaxy 3C28 which is the first ranked galaxy of the cluster A115, already discussed in detail in Feretti *et al.* (1984). These radio galaxies have been observed at 1.4 GHz and 4.9 GHz with the Westerbork Synthesis Radio Telescope (WSRT) and the Very Large Array (VLA).

For A98 and A160 we present here also optical CCD images, taken at the Loiano 152 cm telescope (Bologna). Thanks to the good dynamic range of these images it is possible to study the optical details and their connection with the radio morphology.

Observations and data reduction methods are detailed in section 2. Comments on individual source are presented in section 3, and the results are briefly discussed in the closing section.

In table I the general properties of the clusters are given. A Hubble constant $H_0 = 100$ km/sec Mpc and a deceleration parameter of $q_0 = 1$ are used throughout this paper.

2. Observation and data reduction procedures.

2.1 VLA OBSERVATIONS. — Table II shows the parameters of the observations. Details of the telescope are given by Thompson *et al.* (1980). As primary flux calibrators we observed 3C286 and 3C138. The post-calibration reduction was done with the AIPS software system. The visibility amplitude were checked for deviating amplitudes, which were edited out. A dirty map of the total intensity was produced and CLEANed (Högbom, 1974 ; Clark, 1980). In order to improve the signal to noise ratio the self-calibration technique was used for the data of A115 and A568.

2.2 WSRT OBSERVATIONS. — Table II presents the observational parameters (see Högbom and Brouw, 1974

Send offprint requests to : G. Giovannini.

for a description of the instrument). The flux scale is that of Baars *et al.* (1977), i.e. it is the same of the VLA data. After the calibration, the visibility data were translated into VLA export format and the maps were produced using the AIPS reduction system. The self-calibration technique was successfully applied to the WSRT data.

In order to improve the VLA u-v coverage in the range of the shortest baselines, the WSRT data were added to the VLA visibility points. Since the WSRT data have a larger number of visibility points than VLA data, different weights have been used. All field sources in the WSRT and VLA data have been subtracted in the u-v plane before u-v data concatenation, then a map was obtained.

For comparing maps at different frequencies, the same u-v range and restoring beam were used.

2.3 OPTICAL OBSERVATIONS. — The CCD camera of the Loiano 152 cm telescope (Bologna) has a RCA SID501 detector. The image field is 512 × 320 pixels, each of which is 30 × 30 μ in size with an image scale of 0.53 arcsec/pixel. A red filter was used during the observations, which had an exposure of ~ 10 min. The CCD frames were transported into the AIPS system, where X and Y coordinates were transformed to RA and DEC by means of supplied object positions. The typical position error is of the order of half pixel ; the resolution measured by fitting with a Gaussian some stars present in the fields, is 1.2″-1.4″ (HPBW).

3. The individual radio sources.

3.1 ABELL CLUSTER 98. — The cluster A98 shows in optical a double structure (A98 North and A98 South) with separation of ~ 9′ and probably it is in the process of collapsing before the final relaxation and virialization (Faber and Dressler, 1977 ; Henry *et al.*, 1981 ; Beers *et al.*, 1982).

Observations at X-ray wavelengths with the IPC on board the Einstein satellite indicate a double X-ray emission, similar to the optical distribution of galaxies (Henry *et al.*, 1981 ; Forman *et al.*, 1981). In the center of A98N, a pointlike X-ray source was detected and tentatively identified with the first ranked galaxy of this subcluster (Henry *et al.*, 1981). However, near the subcluster center a flat spectrum radio source (Slingo, 1974) with no optical counterpart (Parma, private communication) is present. This suggests the possibility that the pointlike X-ray source could be a background source associated with the flat spectrum radio source.

The radio emission of A98S is characterized by an extended radio source with double structure, identified with the first ranked galaxy (Owen *et al.*, 1977 ; Fanti *et al.*, 1983b). The map of the radio source obtained with the VLA at 1.4 GHz with a resolution of 4″ is presented in figure 1, superimposed on the CCD image. The total flux in the VLA map is about the 60 % of the 1.4 GHz WSRT total flux (Fanti *et al.*, 1983b), due to the lack of short spacings in the VLA observations. Table III gives the source parameters.

The radio source shows a flat spectrum core coincident with the galaxy and, after a radio gap of ~ 20″ (32 kpc) two nearly symmetric jets and two elongated lobes which can be resolved into smaller substructures. Up to ~ 150 kpc from the core the whole radio structure is well aligned within a few degrees, but shows wiggles and bendings in the jets and a western spread in the southern most region. These substructures may be due to jet instabilities, since no bright companion is present, which could affect the jet propagation through gravitational interaction.

The position of the X-ray centroid is coincident within the errors with the galaxy position ; the thermal pressure of the X-ray gas in the cluster center is $P_x = 5.3 \times 10^{-12}$ dyne/cm^2 (KT = 3 keV ; Forman *et al.*, 1981). The value of the minimum internal energy density in the radio plasmoids allows us to compute the non thermal pressure which is $P_r = 2.6 \times 10^{-12}$ dyne/cm^2 in the jet regions and lower in the outer radio regions. In static conditions there is balance between the two pressures, however with a galaxy velocity larger than 350 km/s, the ram pressure exerted by the ambient gas on the radio plasmoids becomes relevant for the radio source morphology.

The lack of a bent structure of the radio lobes is surprising, due to the high velocity dispersion of the cluster. A high velocity of the galaxy (see Tab. VII) is in agreement with the low stage of evolution of the cluster, but is in contrast with the X-ray centroid being not displaced from the galaxy. It is possible that the X-ray centroid and the galaxy are actually displaced along the line of sight and the radio structure is bent in a direction parallel to the line of sight. This would imply a linear size greater than 500 kpc, which is not unreasonable (see for instance 3C465 (Van Breugel, 1980) and 1919+479 (Robertson, 1984)). A tail structure for this source was also suggested by Owen *et al.* (1977). Another possibility is that the velocity of the radio jet is much higher than the galaxy velocity, leading to negligible effects of the external ram pressure.

3.2 ABELL CLUSTER 115. — A115 is a distant cluster extensively studied at X-ray and optical wavelengths (Beers *et al.*, 1983). The cluster is classified as double on the basis of the IPC X-ray data (Forman *et al.*, 1981), which show two peaks of emission coincident with the two main subcondensations of galaxies. The brightest galaxy of the cluster lies in the northern clump and is identified with the strong radio source 3C28. High resolution and sensitivity radio maps and HRI X-ray data on this source allowed us to study the interaction of the radio source and the ambient gas (Feretti *et al.*, 1984). In

particular, the resolved X-ray structure was interpreted as originating from a hot gas which is likely to be accreting onto the galaxy. The very unusual radio structure, characterized by two components located on both sides of the optical galaxy, with low brightness tails in the western direction, was interpreted as probably due to buoyancy effects. The map presented here (Fig. 2) was obtained at 4.9 GHz with the VLA (C configuration). The radio structure at 4.9 GHz is very similar to that at 1.4 GHz (see Fig. 2 in Feretti *et al.*, 1984). The radio peak positions are coincident in the two maps. In table IV the source radio data are given.

In figure 2 the values of spectral indices, computed between 1.4 GHz and 4.9 GHz, are superimposed on the contour levels. The mean value of the spectral index for component A and B is ~ 2.0 ([1]). In the bridge between the two components the spectral index reaches the highest value. The total spectrum of the source (see Fig. 3) is fairly straight between 38 MHz and 2.7 GHz ($\alpha \sim 1.1$). Between 2.7 GHz and 4.9 GHz the spectral index steepens ($\alpha \sim 2.5$) indicating that the radiation losses are very important in this source. Our 4.9 GHz flux density is in agreement with that obtained by Grueff *et al.* (1981) with a lower resolution and shorter spacings than us, indicating that no missing flux is present in our data.

The polarization map at 4.9 GHz shows two peaks near the total intensity peaks. In the component A the fractional polarization reaches the value of $\sim 9 \pm 2$ % with a position angle of $\sim 60°$; in the component B the maximum is $\sim 8 \pm 2$ % with a position angle of $\sim 25°$. The reanalysis of the 1.4 GHz data (Feretti *et al.*, 1984) showed that the source is unpolarized at this frequency (polarization percentage < 2 %).

As discussed in Feretti *et al.* (1984), the radio source is confined by a dense X-ray gas, which prevents adiabatic losses. This is confirmed by the small extent of the source, despite of its high radio power. This source is a typical case where the lifetime of the radio source might be increased sufficiently for the spectrum to be steepened by synchrotron energy losses of the electrons. Similar cases are discussed by Roland *et al.* (1985). It is expected to find steep spectrum radio galaxies in X-ray clusters, due to the high pressure of the intergalactic medium which allows the steep spectrum sources to survive. The fact that a low percentage of radio sources is found with spectral index $>$ 1-1.5 indicates that the density of the intracluster medium usually is not high enough to prevent the expansion of radio lobes and that radio sources usually suffer significant adiabatic losses in addition to synchrotron ones.

3.3 ABELL CLUSTER 160. — The dominant member of A160 is a galaxy characterized by multiple nuclei or a satellite system. It consists of four optical components whose velocities are 13041 km/sec (East component), 13150 km/sec (West component), 12839 km/sec (South-East component) and 13752 km/sec (North-West component) (Tonry, 1985). The CCD observation is shown in figure 4, superimposed on the VLA radio map obtained at 1.4 GHz. The radio emission is clearly identified with the E component, which is the dominant member of the system.

Due to the large angular extent of this source, the best map has been obtained combining WSRT and VLA data, allowing us to map the whole structure with a HPBW of $5'' \times 5''$. The map is showed in figure 5 and radio data are given in table V. The source appears as a very long collimated two-sided jet with an extension of $\sim 8'$. The northern jet has a pronounced bending to E while the southern lobe has an S shape. The structure of this source is somewhat reminiscent of 3C449 (Cornwell and Perley, 1984) and is probably due to dynamical interaction between the multiple galaxy nuclei. What is impressive in the present source is the very high collimation of the jets and the lack of extended structure. A comparison of the total flux measured in our combined map, with that present in the short WSRT baselines, shows that, despite the resolution of 5″, no extended structure has been lost (see also Fanti *et al.*, 1983a).

In the higher resolution map (Fig. 4) a gap of $\sim 30''$ ($\sim$ 20 kpc) is visible between the core and the brightness peak of the two symmetric and extended jets. Within this gap a fainter jet structure only in the N direction is visible, in spite of the symmetry of the outer regions.

In the 4.9 GHz WSRT map (Fig. 6), the core is more evident, while the total structure is similar to the 1.4 GHz combined map. Along the radio structure some blobs are present.

The spectral index distribution and the brightness at 4.9 GHz in mJy/beam, along the ridge of maximum brightness are shown in figure 7. The spectrum is flat in the core ($\alpha = -0.1$). Along the N jet the spectral index is 0.4-0.6, it becomes ~ 1.0 in the peak of emission, then steepens to ~ 1.7. In the S lobe the spectral index is 0.3-0.5 in the two peaks visible in the 4.9 GHz map and steepens to ~ 1.8 with oscillations (0.8-1.2) where radio blobs are present. It seems that in radio blobs the spectrum is flatter than in the close low brightness regions, probably because reacceleration processes are present. This behaviour of the spectrum is also present in the radio galaxy IC4296 (Killeen *et al.*, 1986).

The analysis of the polarized flux showed that the core is unpolarized at both 1.4 and 4.9 GHz while polarized flux is present along the jet. In table V values of the polarization percentage and of the direction of E vectors in different regions of the source, are given. Note that at 4.9 GHz the polarization vectors are always perpendicular to the direction of the jets therefore the intrinsic magnetic field is parallel to the jet axis along the whole

([1]) $S \propto \nu^{-\alpha}$.

source. This differs from what is usually found for sources of this structure ; longitudinal fields are generally found in one-sided jets of edge brightened sources. NGC 1265 is another source with low power two-sided jets with longitudinal field, this is interpreted as due to strong interaction with the external medium (O'Dea and Owen, 1984). Also in the present source we invoke a viscous interaction with the ambient gas, which is likely to confine the source, preventing the formation of extended structure.

The source is significantly depolarized at 1.4 GHz, with values of depolarization ranging from 0.2 to 0.5. In the case that this is entirely due to internal differential Faraday rotation and the source can be modelled as a slab, the implied R.M. is 64 rad/m^2 and 47 rad/m^2, respectively. Consequently, rotations of 50-65° between the position angles at 1.4 and 4.9 GHz are expected. The polarization vectors at 1.4 GHz are not in agreement with this prediction but show variations on small scale ($\sim$ 10 kpc). We have not computed the trend of the observed rotation measure along the source, since with two frequency measurements, we cannot solve for the $\pm n\pi$ ambiguity ; however, it seems that the RM shows variations on scale of $\sim$ 10 kpc. We conclude that at least part of the rotation occurs in a foreground screen.

3.4 ABELL CLUSTER 278. — A278 contains a head-tail radio source identified with the dominant galaxy in the center of the cluster (Owen *et al.*, 1977). The radio source was mapped by Owen *et al.* (1977) at 2.7 GHz and by Fanti *et al.* (1983a) at 1.4 GHz. In these low resolution maps the source has a length of $\sim$ 200 kpc. High resolution observations have been obtained by O'Dea and Owen (1985) at 4.9 GHz with the VLA (A and C array). They mapped only the inner part of the source, which appears as a one-sided jet. The present map obtained at 1.4 GHz with the VLA (B array) is shown in figure 8. In our map the source has a length of $\sim$ 59 kpc and a total flux density of 260 mJy. The surface brightness is rather uniform with a peak coincident with the optical position and a second one at the end of the jet. The mean spectral index computed between the present 1.4 GHz and the 4.9 GHz C array data of O'Dea and Owen (1985) which have a comparable resolution is quite flat ($\sim$ 0.4). Note that this value refers to the only first 60 kpc of this single tail source.

At 1.4 GHz the core is unpolarized, while in the tail the polarization percentage is 5-7 % $\pm$ 2 % with a not constant position angle orientation. In the peak at the end of the jet the fractional polarization is 4 % $\pm$ 1 % with an angle $\sim$ 40°.

The cluster has been observed at X-ray wavelengths with the IPC on board the Einstein Observatory (Johnson, private communication). A comparison of the radio and X-ray map indicates that the head-tail source is not centered exactly on the X-ray emission. Furthermore the direction of the radio source axis is not aligned with a radius from the center of the IPC image to the head of the radio source.

The discordance between the X-ray centroid and the position of this first ranked galaxy account for its radio morphology. This galaxy is likely to be moving in the cluster potential center within a dense gas.

3.5 ABELL CLUSTER 568. — The cluster of galaxies A568 is characterized by a small group of galaxies located in its center within $\sim 1'$, corresponding to a linear distance of about 65 kpc. The velocity dispersion of this system requires (assuming a homogeneous mass distribution) a total mass of the group of $\sim 3 \times 10^{13}\ M_\odot$ to gravitationally bind the system.

The radio emission of this group was studied by many authors (O'Dea and Owen, 1985 and Ref. therein). The map of O'Dea and Owen (1985), obtained at 1.4 GHz with the VLA (A configuration), shows a very complex structure whose interpretation is still uncertain. O'Dea and Owen (1985) suggested that it probably consists of two interacting radio galaxies.

The WSRT maps at 4.9 GHz and the VLA map (B configuration) at 1.4 GHz are shown in figure 9 and 10 respectively, while radio data are given in table VI. Due to radio source morphology, only total flux densities are given. From a comparison of the WSRT and VLA data at 1.4 GHz, it is evident that no significant extended region is lost in the VLA map.

The radio source in the northern part of the map (« C » in Fig. 9) is another radio galaxy, probably a cluster member. No redshift is at the present available ; see also Fanti *et al.* (1983a).

The WSRT and VLA data at 1.4 GHz have been concatenated to derive the spectral index distribution between 1.4 and 4.9. The values of the spectral index between 4.9 and 1.4 GHz are indicated in figure 9. Typical errors range from ($\sim$ 0.03 in the peaks to $\sim$ 0.1 in the low brightness outer regions).

The present maps and the trend of the spectral index seem to confirm the hypothesis of O'Dea and Owen (1985) that the radio source actually consists of two tail galaxies. The radio galaxy « A » coincides with the strongest peak in the 4.9 GHz and 1.4 GHz maps and has a flat spectrum (0.3). It is likely to be a WAT with an opening angle of at least $\sim$ 90°. The E-W tail is in the same direction as a curved jet starting from the core of the galaxy ; its spectrum steepens at a constant rate, with the spectral index increasing from 1.0 to > 1.7. At the end of the N-S tail there is a feature emerging toward the source axis. The spectrum steepens from the nucleus to the outer region, and is very steep (1.5) in the aforementioned feature.

The second galaxy « B » is the brightest member of the small group. The radio morphology consists of a two

sided jet with a strong bending of the eastern jet towards N-W. The spectral index is 0.6 in the central region has a value of 0.8 in the external lobes, prior to the bending and steepens to ~ 1.2 after the bend. Moreover a diffuse low brightness region, with a very steep spectrum (1.8-2.0), is present north of this source. The low brightness region and the bending of the jet suggest the possibility that this source is a tail source almost along the line of sight. More detailed radio observations are necessary to better map this structure.

While the interaction of a radio galaxy with a companion galaxy is not unusual and its effect on the radio morphology is well known (see for instance 3C31, Strom *et al.*, 1983), the case of two interacting extended radio galaxies is exceptional. It is not clear in the present case if a mutual interaction between the radio plasmons is present and how the radio structure can be influenced. It seems that source A is a usual tail source, while source B could be bent by the tail of source A. The central gas density in this cluster is 1.9×10^{-3} cm^{-3} (Abramopulos and Ku, 1983). Therefore the bent structure is not unexpected considering the high velocity of the individual galaxies and the dense medium. Higher resolution radio polarimetric observations together with new optical and X-ray information will be published elsewhere.

4. Conclusion.

The small sample at our disposal does not allow statistical inferences concerning the properties of first ranked galaxies in clusters. Therefore we make only some general comments.

We present in table VII the relevant radio data on the sources and relevant intrinsic data on the sources and environment. Radio total powers are of intermediate strength, i.e. of the order of 10^{24} W/Hz, except for A115 which is an order of magnitude more powerful.

X-ray data, available for all these clusters except A160, indicate in all cases the presence of a hot intracluster medium ; the density of the gas is particularly high in A115, where a radio source with small linear extent is found, despite the high radio power. This means that the dense gas present in A115 plays a very important role in the confinement of the radio plasmoids, whose stopping distance is strongly reduced. For sources of the same power, one would expect to find a correlation between the linear radio source extent and the gas density. The five present clusters show several radio morphologies : they include an head-tail, an unclassifiably complex structure, one source composed of two interacting wide-angle-tails and two sources with extremely distorted jets. The common property of these sources is the presence of more or less prominent bendings in their morphology, even on different linear scales. It does not seem that the structure of these radiosources associated with first ranked galaxies is different from other cluster radio sources. Fanti (1984) found that 70 % of the cluster sources with linear size larger than 40 kpc show a tail morphology (HT + WAT). By interpreting the bent structures as due to ram pressure exerted by the ambient gas on the radio plasmoids, considerable galaxy velocities must be assumed. While massive first ranked galaxies are believed to be almost at rest in the centers of evolved and relaxed clusters, we can expect that they move at high velocities in clusters at low stage of evolution : this seems to be the present case, since the present clusters are likely to be young and little evolved. We therefore invoke the galaxy motion as the responsible of distorted structures.

It would be interesting to get radio and X-ray information on a big sample of first ranked cluster galaxies, in order to derive the percentage of extended radio sources and the correlation between the radio emission and the properties of the associated clusters.

Acknowledgements.

We thank R. Fanti and S. Spangler for comments and suggestions. Thanks are also due to N. Primavera and V. Albertazzi for the figures. The WSRT is operated by the Netherland Foundation for Radio Astronomy, with the financial support of ZWO. The National Radio Astronomy Observatory is operated by Associated Universities, Inc., under contract with the National Science Foundation.

References

ABRAMOPULOS, F., KU, W. H.-M. : 1983, *Astrophys. J.* **271,** 446.
BAARS, J. W. M., GENZEL, R., PAULINY-TOTH, I. I. K., WITZEL, A. : 1977, *Astron. Astrophys. Suppl. Ser.* **61,** 99.
BEERS, T. C., GELLER, M. G., HUCHRA, J. P. : 1982, *Astrophys. J.* **257,** 23.
BEERS, T. C., HUCHRA, J. P., GELLER, M. G. : 1983, *Astrophys. J.* **264,** 356.
CLARK, B. G. : 1980, *Astron. Astrophys.* **89,** 377.
COLLA, G., FANTI, C., FANTI, R., FICARRA, A., FORMIGGINI, L., GANDOLFI, E., LARI, C., MHARANO, B., PADRIELLI, L., TOMASI, P. : 1972, *Astron. Astrophys. Suppl. Ser.* **7,** 1.
CORNWELL, T., PERLEY, R. : 1984, in « Physics of energy transport in extragalactic radio source » *NRAO workshop,* p. 39.
FABER, S. M., DRESSLER, A. : 1977, *Astron. J.* **82,** 187.

FANTI, C., FANTI, R., FERETTI, L., FICARRA, A., GIOIA, I. M., GIOVANNINI, G., GREGORINI, L., MANTOVANI, F., MARANO, B., PADRIELLI, L., PARMA, P., TOMASI, P., VETTOLANI, G. : 1982, *Astron. Astrophys.* **105,** 200.
FANTI, C., FANTI, R., FERETTI, L., GIOIA, I. M., GIOVANNINI, G., GREGORINI, L., PADRIELLI, L., PARMA, P., TOMASI, P., MARANO, B., ZITELLI, V. : 1983a, *Astron. Astrophys. Suppl. Ser.* **51,** 179.
FANTI, C., FANTI, R., FERETTI, L., GIOIA, I. M., GIOVANNINI, G., GREGORINI, L., PADRIELLI, L., PARMA, P., TOMASI, P., MARANO, B., ZITELLI, V. : 1983b, *Astron. Astrophys. Suppl. Ser.* **52,** 411.
FANTI, R. : 1984, *Clusters and Groups of Galaxies* (Reidel P. C.) p. 185.
FERETTI, L., GIOIA, I. M., GIOVANNINI, G., GREGORINI, L., PADRIELLI, L. : 1984, *Astron. Astrophys.* **139,** 50.
FORMAN, W., BECHTOLD, J., BLAIR, W., GIACCONI, R., VAN SPEYBROECK, L., JONES, C. : 1981, *Astrophys. J. Lett.* **243,** L133.
GRUEFF, G., KOTANYI, C., SCHIAVO-CAMPO, P., TANZELLA-NITTI, G., VIGOTTI, M. : 1981, *Astron. Astrophys. Suppl. Ser.* **44,** 241.
HENRY, J. P., HENRIKSEN, M. J., CHARLES, P. A., THORSTENSEN, J. R. : 1981, *Astrophys. J. Lett.* **243,** L137.
HÖGBOM, J. A. : 1974, *Astron. Astrophys. Suppl. Ser.* **15,** 417.
HÖGBOM, J. A., BROUW, W. N. : 1974, *Astron. Astrophys.* **33,** 289.
KARACHENTESV, I. D., KOPYLOV, A. I. : 1981, *Sov. Astron. Lett.* **7,** 285.
KELLERMANN, K. I., PAULINY-TOTH, I. I. K., WILLIAMS, P. J. S. : 1969, *Astrophys. J.* **157,** 1.
KILLEEN, N. E. B., BICKNELL, G. V., EKERS, R. D. : 1986, *Astrophys. J.* **302,** 306.
O'DEA, C. P., OWEN, F. N. : 1985, *Astron. J.* **90,** 927.
O'DEA, C. P., OWEN, F. N. : 1984 in « Physics of Energy Transport in Extragalactic Radio Sources » p. 47, *NRAO* (Green Bank).
OWEN, F. N., RUDNICK, L., PETERSON, B. M. : 1977, *Astron. J.* **82,** 677.
ROBERTSON, J. G. : 1984, *Astron. Astrophys.* **138,** 41.
ROLAND, J., HANISCH, R. J., VERON, P., FOMALONT, E. : 1985, *Astron. Astrophys.* **148,** 323.
SLINGO, A. : 1974, *Mon. Not. R. Astron. Soc.* **186,** 307.
STROM, R. G., FANTI, R., PARMA, P., EKERS, R. D. : 1983, *Astron. Astrophys.* **122,** 305.
THOMPSON, A. R., CLARK, B. G., WADE, C. M., NAPIER, P. J. : 1980, *Astrophys. J. Suppl. Ser.* **44,** 151.
TONRY, J. L. : 1985, *Astron. J.* **90,** 2431.
ULRICH, M. H. : 1976, *Astrophys. J.* **206,** 364.
VAN BREUGEL, W. J. : 1980, *Astron. Astrophys.* **88,** 248.

TABLE I. — *General properties of the clusters.*

Name	D.C	R	B-M	(V)	(N)	#(V)	REF
A98	5	3	II-III	31593	(14)	1008	1
A115	6	3	III	59015	(8)	1252	2
A160	4	0	III	13288	(8)	1040	3
A278	3	0	III	26460	(1)	-	4
A568	3	0	II-III	22540	(3)	1016	5

PRESENTATION:
Col. 1: Abell name
Col. 2: Distance class
Col. 3: Richness class
Col. 4: Bautz Morgan type
Col. 5: Mean heliocentric velocity of the cluster in km/sec and in parentheses the number of galaxies used to determine it
Col. 6: Velocity dispersion on the line of sight in km/sec
Col. 7: References as below:

1) Beers et al. (1982); the mean and dispersion velocity refer to the southern cluster subcondensation
2) Beers et al. (1983); only subclusters A and B have been used to compute the mean and dispersion velocity
3) Karanchentsev and Kopylov (1981)
4) Fanti et al. (1983a)
5) O'Dea and Owen (1985)

TABLE II. — *Observational summary.*

VLA Observations

Cluster and Source Name	Frequency (MHz)	Bandwidth (MHz)	Observing date	Observing time (min)	Radiotelescope Configuration	Beam (arcsec)	Noise (mJy/beam)
A98							
0043+20	1465	50	August 82	20	B	4.0	0.3
A115							
0053+26 (3C28)	4885	50	April 84	30	C	3.5	0.06
A160							
0110+15	1465	50	August 82	20	B	4.1	0.5
A278							
0154+31	1465	50	August 82	30	B	3.7	0.3
A568							
0704+35	1465	50	August 82	20	B	3.5	0.1

WSRT Observations

Cluster and Source Name	Frequency (MHz)	Bandwidth (MHz)	Observing date	Observing time (hour)	Interferometer Spacing (meter)	Beam (arcsec) RAxDEC	Noise (mJy/beam)
A160							
0110+15	1412	10	June 82	12	72+n72	12.4x53.8	0.4
	4874	80	December 83	12	72+n72	4.1x12.7	0.1
A568							
0704+35	1412	10	August 82	12*	36+n72	12.7x21.8	0.4
	4874	80	December 83	2x12	36+n72 72+n72	3.8x6.0	0.065

* only 30 interferometers

TABLE III. — *Data of 0043+20 (A98).*

	Position RA h m s	Position DEC ° ' "	VLA Flux 1.4 GHz mJy
Optical	00 43 50.71	20 11 41.9	
Radio			
Core	00 43 50.75	20 11 41.6	5.9
N lobe			48
N jet			111
S jet			150
S lobe			46
total			340

TABLE IV. — *Data of 3C28 (A115).*

	Position RA h m s	Position DEC ° ' "	VLA Flux 4.9 GHz mJy
Core	00 53 09.1	26 08 24 *	⟨0.2 $
A	00 53 08.5	26 08 32	56
B	00 53 09.4	26 08 09	57

Note: * RA and DEC refer to the optical position of the galaxy
$ The flux upper limit is in mJy/beam

TABLE V. — *Data of 0110+15 (A160).*

Region	Position RA h m s	Position DEC ° ' "	Flux 1.4 GHz I	1.4 GHz %	1.4 GHz PA	Flux 4.9 GHz I	4.9 GHz %	4.9 GHz PA
Core	01 10 20.13	15 13 35.8	6.3			5.2		
N1				5	82		20	10
N2				20	-86		50	-90
N3				25	-30		50	-85
S1				4	35		20	-70
S2				10	35		50	55
S3				10	-45		35	20
S4				15	85		60	-89
Total			1064			231		

PRESENTATION:
Col. 1: Regions of the source named as in Fig. 6
Col. 2,3: Radio position of the core from the 4.9 GHz map
Col. 4,7: Total intensity flux in mJy at 1.4 and 4.9 GHz respectively
Col. 5,8: Polarization percentage at 1.4 and 4.9 GHz respectively
Col. 6,9: Position angle in degree of E vectors at 1.4 and 4.9 GHz respectively

TABLE VI. — *Data of 0704+35 (A568).*

	1.4 GHz	4.9 GHz	
WSRT	381	118	mJy
VLA	388		mJy

TABLE VII. — *Radio source and cluster data.*

	P Core (5 GHz) x 10^{21} W/Hz	P tot (1.4 GHz) x 10^{24} W/Hz	Size kpc	Central gas density x 10^{-3} cm^{-3}	Vcl-Vgal km/sec
A98 0043+20	45.4	6.6	305	1.1	604
A115 0053+26 (3C28)	(8.4	58.1	85	43	770
A160 0110+15	11.0	2.2	290	*	247
A278 0154+31	11.7	3.1	~200	yes $	-
A568 0704+35	146 and (9.1	3.0	~100	1.9	430 and 1160

Notes
*: not published; $: Johnson, private comunication
Total powers at 1.4 GHz are computed from literature data (to include low brightness regions). Core powers at 5 GHz are from present data, except for A98 (extrapolated) and A278 (O'Dea and Owen, 1985). For A568 Pc and Vcl-Vgal refers to galaxies A and B respectively.

PRESENTATION:
Col. 1: Cluster and source name
Col. 2: Core radio power at 4.9 GHz in W/Hz
Col. 3: Total radio power at 1.4 GHz in W/Hz
Col. 4: Maximum linear size in kpc
Col. 5: Central gas density from X-Ray data
Col. 6: Difference between the mean cluster velocity (see Tab. 1) and the velocity of the radio galaxy in km/sec

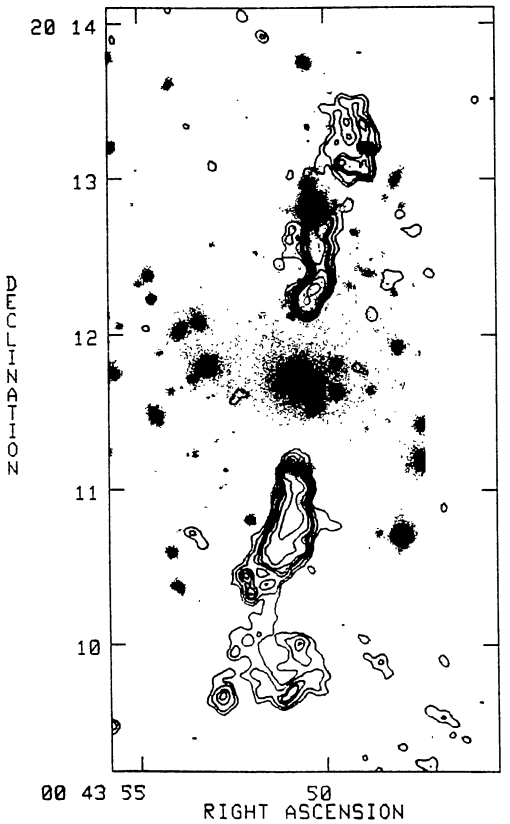

FIGURE 1. — 0043+20 (A98) : Isocontour map obtained with the VLA at 1.4 GHz, superimposed on the optical map obtained with a CCD camera (grey levels). Contour levels are 0.5, 0.8, 1.3, 1.6, 2.0, 3.0, 5.0, 10.0 mJy/beam area. The HPBW is 4″ and 1.3″ for the radio and optical map respectively.

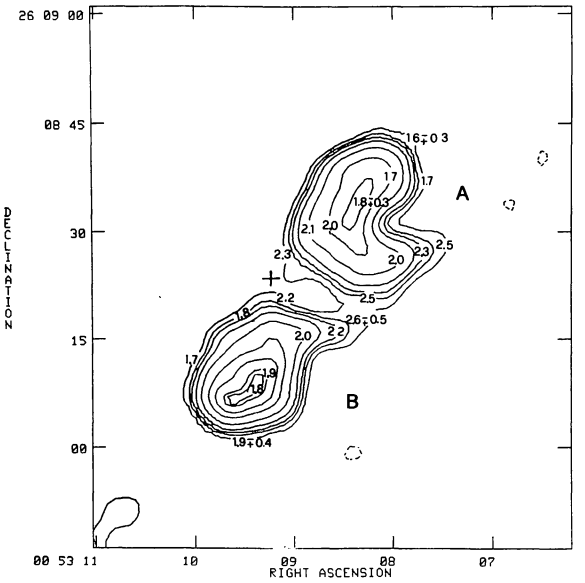

FIGURE 2. — 0053+26/3C28 (A115) : Isocontour map obtained with the VLA at 4.9 GHz. Contour levels are – 0.2, 0.2, 0.4, 0.6, 1.0, 2.0, 4.0, 6.0, 8.0, 8.5 mJy/beam area. The cross marks the optical position. The values of spectral indices, computed between 1.4 GHz and 4.9 GHz, are superimposed on the contour levels. The HPBW is 3.5″.

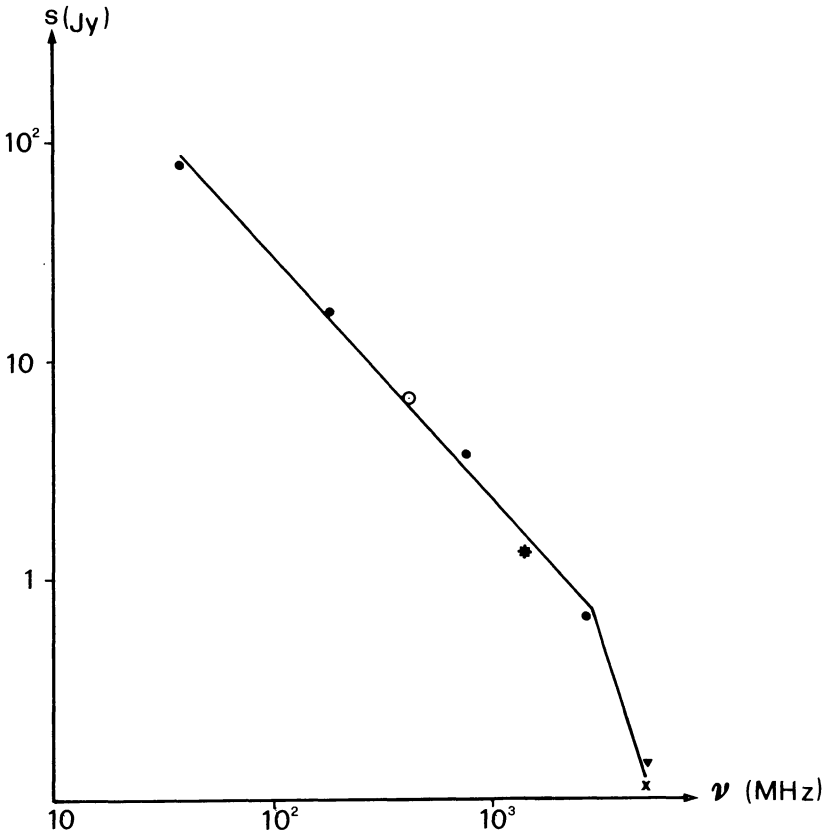

FIGURE 3. — 0053+26/3C28 (A115) : Radio spectrum between 38 MHz and 4.9 GHz. Data are taken from : • Kellerman *et al.* (1969) ; ○ Colla *et al.* (1972) ; ∗ Feretti *et al.* (1984) ; ▼ Grueff *et al.* (1981) ; × Present paper.

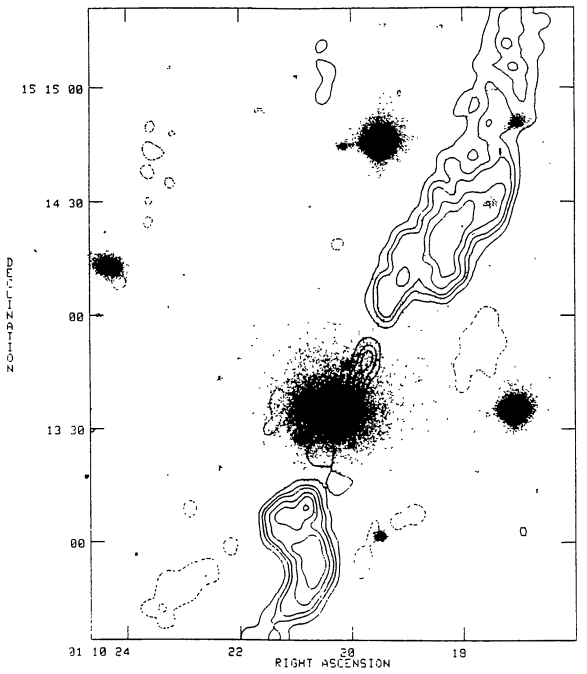

FIGURE 4. — 0110+15 (A160) : Isocontour map obtained with the VLA at 1.4 GHz, superimposed to the optical map obtained with a CCD camera (grey levels). Contour levels are – 1.0, 1.0, 2.0, 3.0, 5.0, 7.0, 10.0 mJy/beam area. The HPBW is 4.1″ and 1.2″ for the radio and optical map respectively.

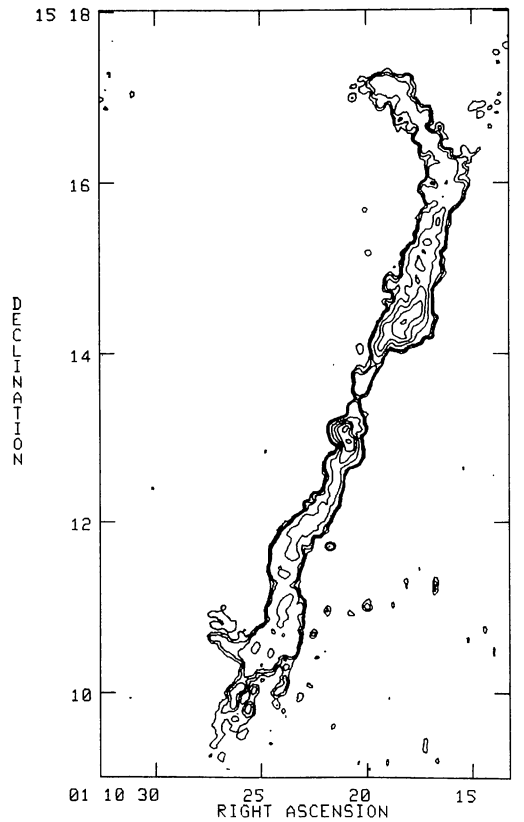

FIGURE 5. — 0110+15 (A160) : Isocontour map obtained combining VLA and WSRT data at 1.4 GHz. Contour levels are – 0.6, 0.5, 0.7, 1.0, 2.5, 5.0, 8.0, 10.0, 12.0 mJy/beam area. The HPBW is 5″.

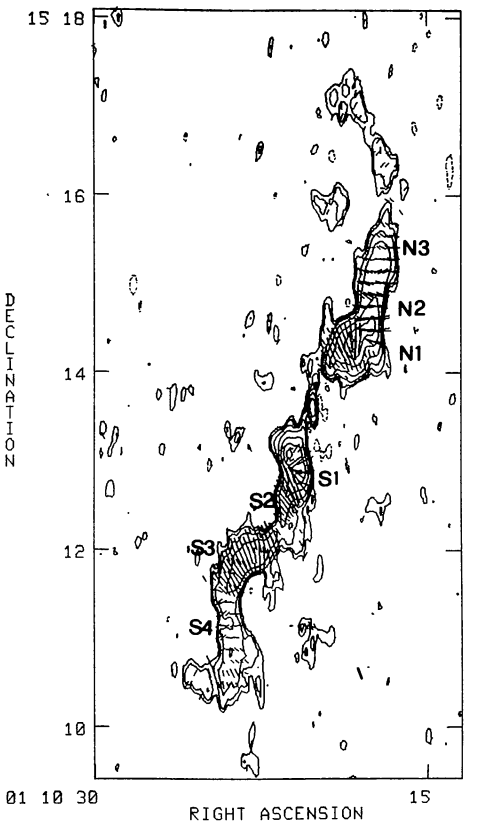

FIGURE 6. — 0110+15 (A160) : Isocontour map obtained with the WSRT at 4.9 GHz. Contour levels are – 0.3, 0.2, 0.3, 0.5, 1.0, 2.5, 5.0, 7.5 mJy/beam area. Line segments, whose length is proportional to the polarized intensity (1′ ~ 4 mJy/beam), indicate the orientation of the E field. Regions for which radio data are given in table V are indicated. The HPBW is 4.1″ × 12.7″ (RA × DEC).

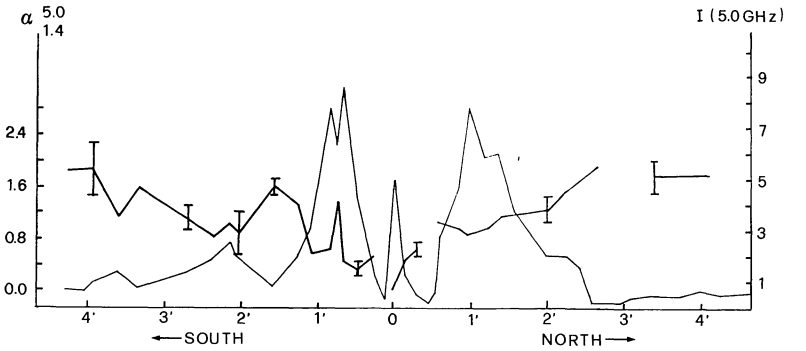

FIGURE 7. — 0110+15 (A160) : Spectral index between 1.4 and 4.9 GHz (heavy line ; segments are 1 r.m.s.) along the line of maximum brightness with the brightness I at 4.9 GHz (in mJy/beam) along the same ridge line shown for reference.

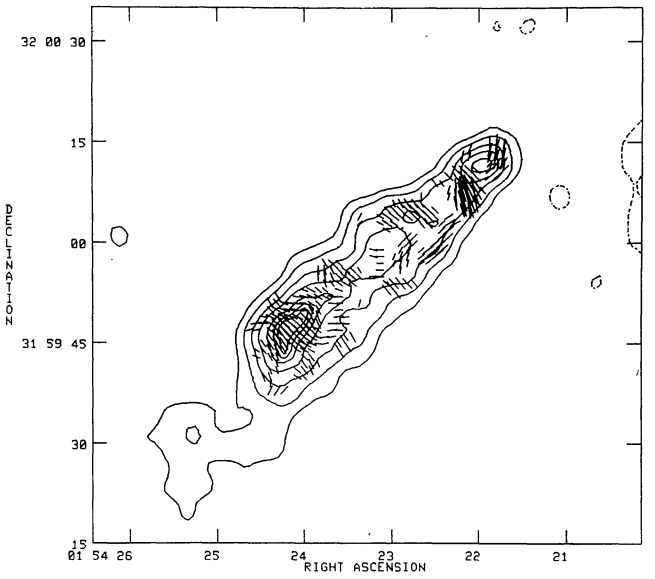

FIGURE 8. — 0154+31 (A278) : Isocontour map obtained with the VLA at 1.4 GHz. Contour levels are – 0.8, 0.8, 2.0, 4.0, 6.0, 8.0, 9.0, 9.5 mJy/beam area. Line segments whose length is proportional to the polarized flux (1′ ~ 8 mJy) indicate the orientation of the E field. The HPBW is 3.7″.

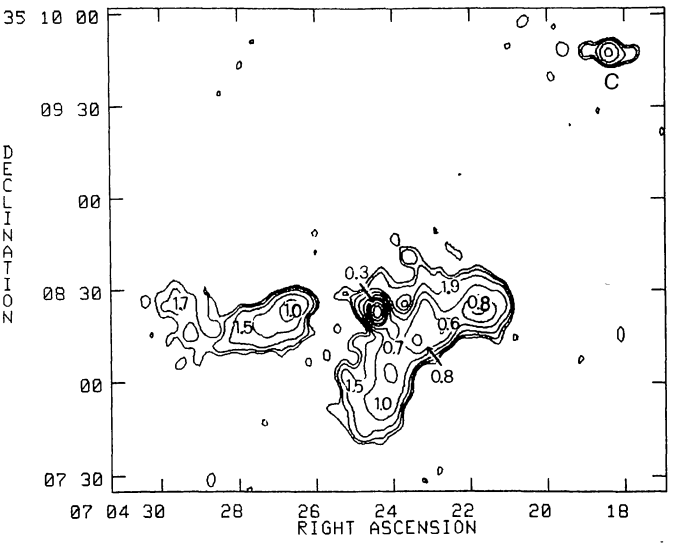

FIGURE 9. — 0704+35 (A568) : Isocontour map obtained with the WSRT at 4.9 GHz. Contour levels are – 0.3, 0.2, 0.3, 0.5, 1.0, 2.0, 4.0, 6.0, 10.0, 15.0 mJy/beam area. The values of spectral indices, computed between 1.4 GHz and 4.9 GHz, are superimposed on the contour levels. The HPBW is 3.8″ × 6.0″ (RA × DEC).

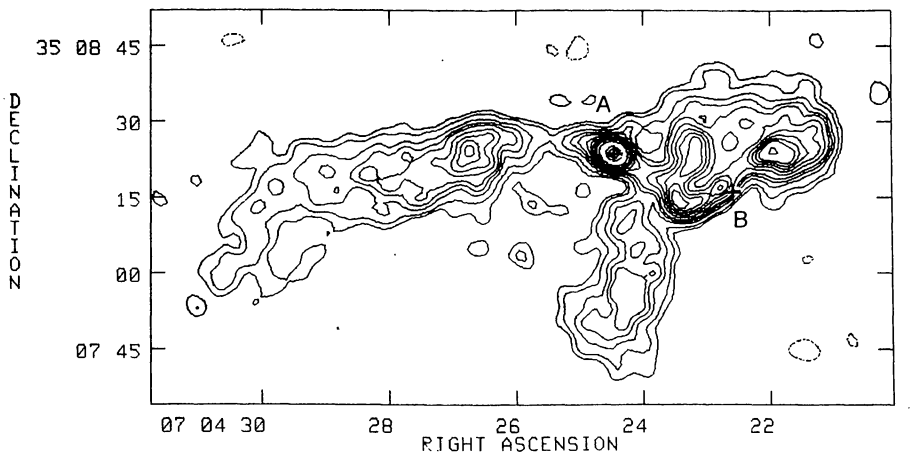

FIGURE 10. — 0704+35 (A568) : Isocontour map obtained with the VLA at 1.4 GHz. Contour levels are – 0.3, 0.3, 0.5, 1.0, 1.5, 2.0, 3.0, 4.0, 5.0, 6.0, 7.0, 10.0, 20.0, 25.0 mJy/beam area. Crosses mark the position of the optical galaxies discussed in the text. The HPBW is 3.5″.